The Journal of Immunology

Leukocyte Infiltration, But Not Neurodegeneration, in the CNS of Transgenic Mice with Astrocyte Production of the CXC Chemokine Ligand 10

Kaan Boztug, Monica J. Carson, Ngan Pham-Mitchell, Valérie C. Asensio, Julie DeMartino and Iain L. Campbell

J Immunol 2002; 169:1505-1515; ;
doi: 10.4049/jimmunol.169.3.1505
http://www.jimmunol.org/content/169/3/1505

The Journal of Immunology is published twice each month by
The American Association of Immunologists, Inc.,
1451 Rockville Pike, Suite 650, Rockville, MD 20852

Print ISSN: 0022-1767 Online ISSN: 1550-6606.

Leukocyte Infiltration, But Not Neurodegeneration, in the CNS of Transgenic Mice with Astrocyte Production of the CXC Chemokine Ligand 10[1]

Kaan Boztug,* Monica J. Carson,† Ngan Pham-Mitchell,* Valérie C. Asensio,[2]* Julie DeMartino,‡ and Iain L. Campbell[3]*

The CXC chemokine ligand (CXCL)10 is induced locally in the CNS in diverse pathologic states. The impact of CXCL10 production in the CNS was examined in transgenic mice with astrocyte-directed production of this chemokine. These glial fibrillary acidic protein (GF)-CXCL10 transgenic mice spontaneously developed transgene dose- and age-related leukocyte infiltrates in perivascular, meningeal, and ventricular regions of the brain that were composed of, surprisingly, mainly neutrophils and, to a lesser extent, T cells. No other overt pathologic or physical changes were evident. In addition, the cerebral expression of a number of inflammation-related genes (e.g., cytokines) was not significantly altered in the transgenic mice. The extent of leukocyte recruitment to the brain could be enhanced markedly by peripheral immunization of GF-CXCL10 mice with CFA and pertussis toxin. This was paralleled by a modest, transient increase in the expression of some cytokine and chemokine genes. Analysis of the expression of the CXCL10 receptor, CXCR3, by the brain-infiltrating leukocytes from immunized GF-CXCL10 transgenic mice revealed a significant enrichment for CXCR3-positive cells in the CNS compared with spleen. The majority of cells positive for CXCR3 coexpressed CD3, whereas Gr1-positive granulocytes were negative for CXCR3 expression. Thus, while astrocyte production of CXCL10 can promote spontaneous and potentiate immune-induced recruitment of leukocytes to the CNS, this is not associated with activation of a degenerative immune pathology. Finally, the accumulation of neutrophils in the brain of GF-CXCL10 transgenic mice is apparently independent of CXCR3 and involves an unknown mechanism. ***The Journal of Immunology*****, 2002, 169: 1505–1515.**

The IFN-inducible non-glutamine-leucine-arginine (ELR)[4] CXC chemokine ligand (CXCL)10 (previously known as IFN-inducible protein 10 and the murine homolog CRG-2) is a secreted polypeptide with a molecular mass of 8.7 kDa (1–3), which is known to be a potent chemoattractant for Th1 T cells, NK cells, and monocytes/macrophages (4–6). In addition to its role in mediating leukocyte chemotaxis, CXCL10 has been shown to exert antiviral (7) and antibacterial (8) activity and is a potent angiostatic factor (9–11). Evidence suggests the angiostatic actions of CXCL10 account, in part, for the marked antitumoral effects of this chemokine (12, 13). Thus, CXCL10 is a plurifunctional chemokine that acts on diverse cell types.

CXCL10 signals through the G protein-coupled seven-transmembrane-spanning receptor CXCR3. This receptor also binds the other two members of the IFN-inducible non-ELR CXC chemokine subgroup, CXCL9 and CXCL11, as well as (in mice but not in humans) the CC chemokine CCL21 (6, 14–17). The preferential expression of CXCR3 on Th1 T cells links the ligands and this receptor to type 1 immune responses (5, 18) and suggests an important role in the development of a variety of inflammatory conditions associated with cellular immune responses. In support of this, a significant abrogation in the tissue accumulation of activated T cells is found in mice with *Toxoplasma gondii* infection (19) or with cardiac allografts (20), following neutralization of CXCL10 or gene-targeted disruption of CXCR3, respectively. Recently, an alternative functional high-affinity receptor for CXCL10, but not CXCL9 or CXCL11, has been found on epithelial and endothelial cells (21); however, cloning and more detailed analysis will be necessary to determine the function of this putative alternative receptor in mediating the actions of CXCL10 in vivo.

CXCL10 is also implicated in the pathogenesis of a variety of neuroinflammatory disorders. In the human CNS, increased CXCL10 levels were reported in many senile plaque-associated astrocytes in Alzheimer's disease (22), while in active multiple sclerosis CXCL10 was found to be increased in cerebrospinal fluid (CSF) (23) as well as to be expressed by astrocytes present in active but not inactive demyelinating lesions (24). High levels of CXCL10 were detected in the CSF of individuals with HIV-1 infection (25) and in astrocytes in brain from individuals with HIV-1-associated dementia (HAD) (26). A significant correlation was found between expression

Departments of *Neuropharmacology and †Molecular Biology, The Scripps Research Institute, La Jolla, CA 92037; and ‡Department of Immunology Research, Merck Research Laboratories, Rahway, NJ 07065

Received for publication March 19, 2002. Accepted for publication May 29, 2002.

The costs of publication of this article were defrayed in part by the payment of page charges. This article must therefore be hereby marked *advertisement* in accordance with 18 U.S.C. Section 1734 solely to indicate this fact.

[1] This work was supported by U.S. Public Health Service Grants MH 62231 and MH 62261 (to I.L.C.). K.B. was supported by a fellowship of the Studienstiftung des Deutschen Volkes. V.C.A. was a postdoctoral fellow of the National Multiple Sclerosis Society. This is manuscript number 14768-NP from the Scripps Research Institute.

[2] Current address: Digital Gene Technologies, La Jolla, CA 92037.

[3] Address correspondence and reprint requests to Dr. Iain L. Campbell, Department of Neuropharmacology, SP-315, The Scripps Research Institute, 10550 North Torrey Pines Road, La Jolla, CA 92037. E-mail address: icamp@scripps.edu

[4] Abbreviations used in this paper: ELR, glutamine-leucin-arginine; CXCL, CXC chemokine ligand; HAD, HIV-1-associated dementia; EAE, experimental autoimmune encephalomyelitis; GFAP, glial fibrillary acidic protein; LCMV, lymphocytic choriomeningitis virus; MHV, mouse hepatitis virus; MMP, matrix metalloproteinase; TIMP, tissue inhibitor of MMP; PTX, pertussis toxin; ECM, extracellular matrix; RPA, RNase protection assay; CSF, cerebrospinal fluid GF, glial fibrillary acidic protein.

0022-1767/02/$02.00

of CXCL10 and the progression of neuropsychiatric impairment, implicating CXCL10 in the pathogenesis of HAD (25). In both HAD (25) and viral meningitis cases (27) CXCL10 in CSF was shown to promote mononuclear cell chemotaxis in vitro.

Extensive analysis of CXCL10 expression in the CNS has been performed experimentally in rodents where significant induction in the CNS levels of this chemokine occur in diverse neuropathologic states, including the inflammatory demyelinating disease experimental autoimmune encephalomyelitis (EAE) (28–32); viral diseases induced by lymphocytic choriomeningitis virus (LCMV) (33, 34), mouse hepatitis virus (MHV) (35), and Theiler's murine encephalomyelitis virus (36, 37); contusion injury (38); cerebral ischemia (39); neurotoxicant-induced neurodegeneration (40); HIV-gp120-induced neurodegeneration (41); and scrapie spongioform encephalopathy (42). Temporal studies in EAE (28, 31, 43) and CNS infection with LCMV (33, 34) or MHV (35) show that the expression of CXCL10 occurs early and parallels the duration and severity of clinical disease. In particular, in the viral models, the induction of CXCL10 in the CNS occurs before detectable leukocyte infiltration and development of clinical disease (33–35). The fact that early induction of CXCL10 precedes leukocyte infiltration suggested that parenchymal brain cells might be responsible for the production of this chemokine. Indeed, this is the case; astrocytes, microglia, and neurons are all local sources for CXCL10 production in, e.g., EAE (29), LCMV infection (34), and MHV infection (35). These experimental studies illustrate the dynamic nature of CXCL10 gene expression in diverse neuropathologic states in which neural cells themselves serve as early and sensitive cellular monitors of perturbation in the brain responding with robust production of CXCL10.

The possible function of CXCL10 in some of these experimental neuropathologies has been explored by recent Ab neutralization studies (44–46). In EAE, administration of anti-CXCL10 decreased clinical and histological disease incidence and severity, and infiltration of mononuclear cells into the CNS. Anti-CXCL10 treatment did not affect the activation of encephalitogenic T cells or their effector function. These studies suggest that CXCL10 has a primary role in the recruitment and accumulation of inflammatory mononuclear cells during the pathogenesis of EAE. Essentially similar conclusions were reached by Liu et al. (45), who demonstrated that neutralization of CXCL10 during MHV encephalitis led to a significant reduction in $CD4^+$ and $CD8^+$ T cell infiltration into the CNS. However, this reduction in CNS cellular immunity severely compromised the host antiviral response, as evidenced by increased CNS viral loads and mortality. Thus, CXCL10 may play a pivotal positive role in the development of the CNS protective immune response to MHV. However, the function of this chemokine may be detrimental in the chronic demyelinating stage of MHV encephalitis because neutralization of CXCL10 reduced inflammatory mononuclear cell accumulation and demyelination and neurologic impairment (44). In all, these findings highlight the central role of CXCL10 in recruiting activated T cells to the CNS during type I immune responses. Interestingly, they also highlight disease stage-related differences in the outcome of this CXCL10-driven process.

As outlined above, it is clear that CXCL10 is a multifunctional chemokine. In view of this, we have hypothesized that the functions of CXCL10 in the CNS may well go beyond leukocyte trafficking. However, at present we know little about what these functions might be and we lack appropriate models for examining this. Accordingly, in this work we have addressed this issue using a well-documented and -characterized transgenic approach (47, 48), in which expression of the murine CXCL10 gene was targeted to astrocytes in the CNS of mice via the use of a glial fibrillary acidic protein (GFAP)-fusion gene construct. As indicated above, astrocytes represent a significant cellular source for the production of CXCL10; therefore, this cell is unquestionably an appropriate and relevant target for the transgene-targeted expression of this chemokine gene.

Materials and Methods

Animals

The methods used for the generation of transgenic mice with astrocyte-targeted gene expression under the transcriptional control of a GFAP promoter was described in detail previously (49, 50). In brief, the coding sequence for the murine CXCL10 gene (bases 33–399; GenBank accession no. M86829) was amplified by RT-PCR from RNA isolated from the brain of LCMV-infected mice. This source of RNA was shown previously to contain high levels of CXCL10 transcripts (33). The following oligonucleotide primers were used for the PCR: $CXCL10^+$, 5′-AGCCAACCT TCCGGAAGCCTCCCCAT-3′; $CXCL10^-$, 5′-ATCACAGCACCGGGG TGTGTGCGTGGCT-3′.

After digestion with the appropriate restriction enzymes and subsequent sequence verification, the amplified CXCL10 cDNA fragment was cloned into a GFAP expression vector (51) containing a human growth hormone polyadenylation signal sequence downstream of the insert. The resulting fusion gene construct was microinjected into the germline of C57BL/6 mice. Genotyping of the animals was accomplished by PCR analysis of genomic tail DNA using primers targeted at the human growth hormone sequence included in the transgene construct. Breeding of the transgenic founder mice and their offspring as well as wild-type littermates was maintained on the C57BL/6 background.

C57BL/6 wild-type mice infected intracranially with LCMV and euthanized on day 6 postinjection (33), as well as 2- to 3-mo-old symptomatic glial fibrillary acidic protein (GF)-IFNα transgenic mice from the GIFN-39 line (52), served as positive controls in various experiments throughout this study.

All mice were maintained under pathogen-free conditions in the closed breeding colony of The Scripps Research Institute (La Jolla, CA).

RNA preparation

Transgenic or wild-type mice were euthanized and their organs were removed, snap-frozen in liquid nitrogen, and stored at −80°C pending RNA extraction. $Poly(A)^+$ RNA was isolated according to a previously described method (53). Total RNA was extracted using TRIzol reagent (Life Technologies, Grand Island, NY) according to the manufacturer's instructions. RNA concentrations were determined by UV spectroscopy at 260 nm.

RNase protection assay

The development and characterization of multiprobe RNase protection assay (RPA) probe sets was described in detail previously (54). Probe sets used throughout this study included the cytokine probe sets ML11 and ML26 (55, 56) (kindly provided by Dr. M. Hobbs, The Scripps Research Institute), the matrix metalloproteinase (MMP) and tissue inhibitor of MMPs (TIMP) probe sets (57), the CNS inflammation probe set (58), the IFN-regulated gene set (41), and the chemokine 1 probe set (33). An additional chemokine multiprobe set (chemokine 2) as well as a CXCR3 probe were constructed with specific details listed in Table I. All RPAs were performed as described previously (54). For quantitation, autoradiographs were scanned and analyzed by densitometry using NIH 1.57 software.

Table I. *cDNA target sequences used to derive the RPA probes*

Target Gene	Sequence	Length (bp)	GenBank Accession No.
Chemokine 2			
CXCL9	101–402	302	M34815
CCL12	65–304	240	U50712
CXCL12	567–777	211	M58004
CCL21	267–444	178	U88322
CXCL1	119–288	170	J04596
CCL11	87–234	148	U40672
CXCL5	301–432	132	U27267
CX3CL1	147–260	114	AF010586
CXCR3	29–188	160	AF045146

Immunoblot analysis

Mice were anesthetized and perfused with ice-cold saline. Brain and peripheral organs were removed and solubilized in an excess volume of lysis buffer (1% IGEPAL-630 (Sigma-Aldrich, St. Louis, MO), one Complete Mini protease inhibitor mixture tablet (Roche, Indianapolis, IN) in 10 ml PBS (pH 7.4)). Following solubilization, the samples were clarified by centrifugation at 10,000 × *g* for 15 min. The supernatant was kept as the cytoplasmic protein fraction and used for immunoblot analysis. Protein concentration was determined using a commercially available protein assay (Bio-Rad, Hercules, CA) used according to the manufacturer's instructions. Protein lysates were stored at −80°C pending further analysis.

Protein samples were denatured under reducing conditions and fractionated electrophoretically on a 10% bis-Tris polyacrylamide gel (Invitrogen, Carlsbad, CA) at 150 V. Following electrophoresis, proteins were transferred to a nitrocellulose membrane, blocked, and then incubated with a polyclonal rabbit anti-murine CXCL10 Ab (PeproTech, Rocky Hill, NJ) or a polyclonal goat anti-human CXCR3 Ab (Research Diagnostics, Flanders, NJ), respectively. Recombinant murine CXCL10 protein (R&D Systems, Minneapolis, MN) served as a positive control in the immunoblots for CXCL10. For quantitation, bands were scanned and analyzed by densitometry using NIH 1.57 software.

Routine histology, in situ hybridization, and immunohistochemistry

For routine histology, animals were anesthetized and perfused transcardially with ice-cold saline and 4% paraformaldehyde in PBS (pH 7.4). Brains were removed and postfixed in the same fixative overnight, processed, and embedded in paraffin. Sagittal sections (5 μm) were cut onto polylysine-coated slides and used for routine staining and in situ hybridization.

In situ hybridization was performed as described previously with modifications (41). For probe, an *Xba*I linearized pGEM4Z (Promega, Madison, WI) plasmid vector containing a 726-bp cDNA fragment of the murine CXCL10 gene was used (33). Antisense ^{33}P-labeled CXCL10 probe was synthesized as described previously (33). Following hybridization and washing, some sections were immunostained for GFAP. For this procedure, slides were incubated in 5% normal goat serum in PBS (pH 7.4) to decrease nonspecific binding, after which the primary Ab (rabbit anti-cow GFAP diluted 1/2000; DAKO, Carpinteria, CA) was applied. Specific binding was detected using biotinylated goat anti-rabbit IgG Ab (Zymed Laboratories, San Francisco, CA), followed by application of an avidin biotinylated HRP complex (ABC) kit (Vector Laboratories, Burlingame, CA) according to the manufacturer's instructions. Staining reactions were performed with a 3,3-diaminobenzidine kit (Vector Laboratories) in the absence of nickel chloride. Stained and unstained slides were dehydrated in a series of graded ethanols, dried, and exposed to Biomax MR film (Kodak, New York, NY) for 4 days. Slides were then dipped in NTB-2 autoradiography emulsion (Kodak), dried, and stored in the dark at 4°C for 3 wk, after which slides were developed, counterstained in hematoxylin for 30 s, and examined by bright field microscopy.

For immunophenotyping and immune accessory molecule immunostaining, mice were anesthetized and perfused transcardially with ice-cold saline. Brains were removed, divided along the sagittal midline, embedded in OCT compound (Sakura Finetek, Torrance, CA), and stored at −80°C until cryosections were cut. Cryosections of 8-μm thickness were equilibrated at room temperature, fixed in ice-cold acetone:methanol (1:1) for 45 s, rinsed in PBS (pH 7.4), and blocked for 30 min in 5% normal goat serum in PBS. The following primary Abs were used: CD4 (L4T3), CD8a (Ly2), CD45 (Ly5), CD106 (VCAM-1) (all from BD PharMingen, San Diego, CA); ICAM-1 (kindly provided by Dr. F. Takei, Terry Fox Laboratory, British Columbia Cancer Research Centre, Vancouver, Canada); neutrophil (7/4; Serotec, Raleigh, NC); Gr1 (RB6-8C5; Caltag Laboratories, Burlingame, CA); fibronectin (Sigma-Aldrich); and Mac-1 (clone TIB126) and MHC class II (clone M5/114; both from the American Type Culture Collection, Manassas, VA). All Abs were used at a final concentration of 5 μg/ml in blocking buffer. Bound Ab was detected using biotinylated anti-rat and biotinylated anti-rabbit secondary Abs (Zymed Laboratories), followed by application of an ABC kit (Vector Laboratories) according to the manufacturer's instructions. Staining reactions were performed with a 3,3-diaminobenzidine kit (Vector Laboratories) in the presence of nickel chloride. Slides were counterstained with hematoxylin and examined by bright field microscopy.

Peripheral immunization with CFA

Transgenic mice (2 mo of age) and wild-type littermates were actively immunized with CFA and boosted with pertussis toxin (PTX) as described previously (59). Following immunization, all mice were observed daily for signs of neurological disease and euthanized at various time points for RNA expression and histological analysis performed as described previously (59).

Leukocyte isolation from spleen and brain

For splenic leukocyte isolation, spleens were removed from wild-type mice and placed in phenol red-free, serum-free HBSS (Sigma-Aldrich). A single-cell suspension was obtained by cutting the organ into small pieces, dispersing the clumps through a 19.5-gauge needle, and expelling the suspension through a 70-μm cell strainer. Cells were pelleted and RBC were lysed in hypotonic lysis buffer (0.15 M NH_4Cl, 1 mM $KHCO_3$, 0.1 mM Na_2EDTA (pH 7.4)). Cell viability was monitored by trypan blue exclusion test and was routinely >95%.

Leukocytes infiltrating the CNS were isolated as described previously with minor modifications (60, 61). In brief, animals were euthanized by halothane inhalation and perfused with 20 ml of PBS (pH 7.4). Brains were rapidly removed and dissociated mechanically by sequentially forcing the tissue through 210- and 70-μm Nitex meshes. The resultant cell suspension was thereafter enzymatically digested with DNase I (28 U/ml) and collagenase (0.2 mg/ml) in HBSS for 1 h at 37°C in a shaking incubator. After quenching the digestion with the addition of 10% FCS (final concentration), the cell suspension was separated on a discontinuous 1.033/1.088/1.122 Percoll (Amersham Pharmacia Biotech, Piscataway, NJ) gradient. Leukocytes were collected from the interface and the 1.033 Percoll fraction. Myelin and cell debris separated above the gradient.

Flow cytometry

Cells were resuspended for 30 min in phenol red-free HBSS with 5% normal goat serum containing FcBlock (BD PharMingen) at a concentration of 0.1 $\mu g/10^6$ cells and thereafter transferred to round-bottom 96-well plates (Corning, Corning, NY). FITC-conjugated Abs used were as follows: 7/4 (Serotec), Gr1 (Caltag Laboratories), and CD3ϵ (145-2C11; BD PharMingen). A rabbit polyclonal anti-CXCR3 Ab (J. DeMartino, unpublished observation) raised against the murine CXCR3 peptide, (NH2)-YLEVSERQVLDASDFAF-Orn-C-OH, representing N-terminal receptor residues 2–18, was used for the analysis of cell surface CXCR3 expression. The specificity of this Ab for CXCR3 was confirmed (J. DeMartino, unpublished observation) by assessing by flow cytometry its ability to recognize Chinese hamster ovary or rat basophilic leukemia cells when transfected with the relevant receptor. In addition, the relevant, but not an irrelevant, peptide blocked Ab binding. Finally, the antisera also neutralized the binding of radiolabeled CXCL10 to murine CXCR3 transfected cells and primary activated murine T cells.

Primary Abs and their corresponding isotype-matched control Abs were reacted for 60 min with the cell suspensions obtained from the Percoll gradient and spleen single-cell suspension, respectively. Following washes in blocking buffer, PE-conjugated donkey anti-rabbit Ab (Jackson ImmunoResearch Laboratories, West Grove, PA) was applied in a 1/100 dilution for 30 min to detect specific binding of the rabbit anti-murine CXCR3 Ab. Stained cells were analyzed on a FACScan flow cytometer (BD Biosciences, Mountain View, CA). Data analysis was performed using WinMDI 2.8 software (The Scripps Research Institute).

Results

Generation of GFAP-CXCL10 transgenic mice and analysis of transgene expression

To generate mice that express the CXCL10 gene in the CNS, we used a well-characterized approach that targets the expression of transgenes to astrocytes (62). Two independent, stable lines of transgenic animals designated GF-CXCL10-2 and GF-CXCL10-10 were established. Animals up to 1 year of age from either of the transgenic lines bred normally and did not show obvious physical or behavioral abnormalities.

Analysis of transgene expression by RPA showed that CXCL10 mRNA transcripts were readily detectable at low levels in brain, spinal cord, and eyes from GF-CXCL10-2 mice and at significantly higher levels in these CNS tissues from GF-CXCL10-10 mice, respectively (Fig. 1, *A* and *B*). While CXCL10 gene expression was not detectable in brain from wild-type controls, it was present at low levels in spinal cord and eye. Notably, CXCL10 gene expression in GF-CXCL10-10 brain was lower than or comparable to levels found in the brain of mice with LCMV infection

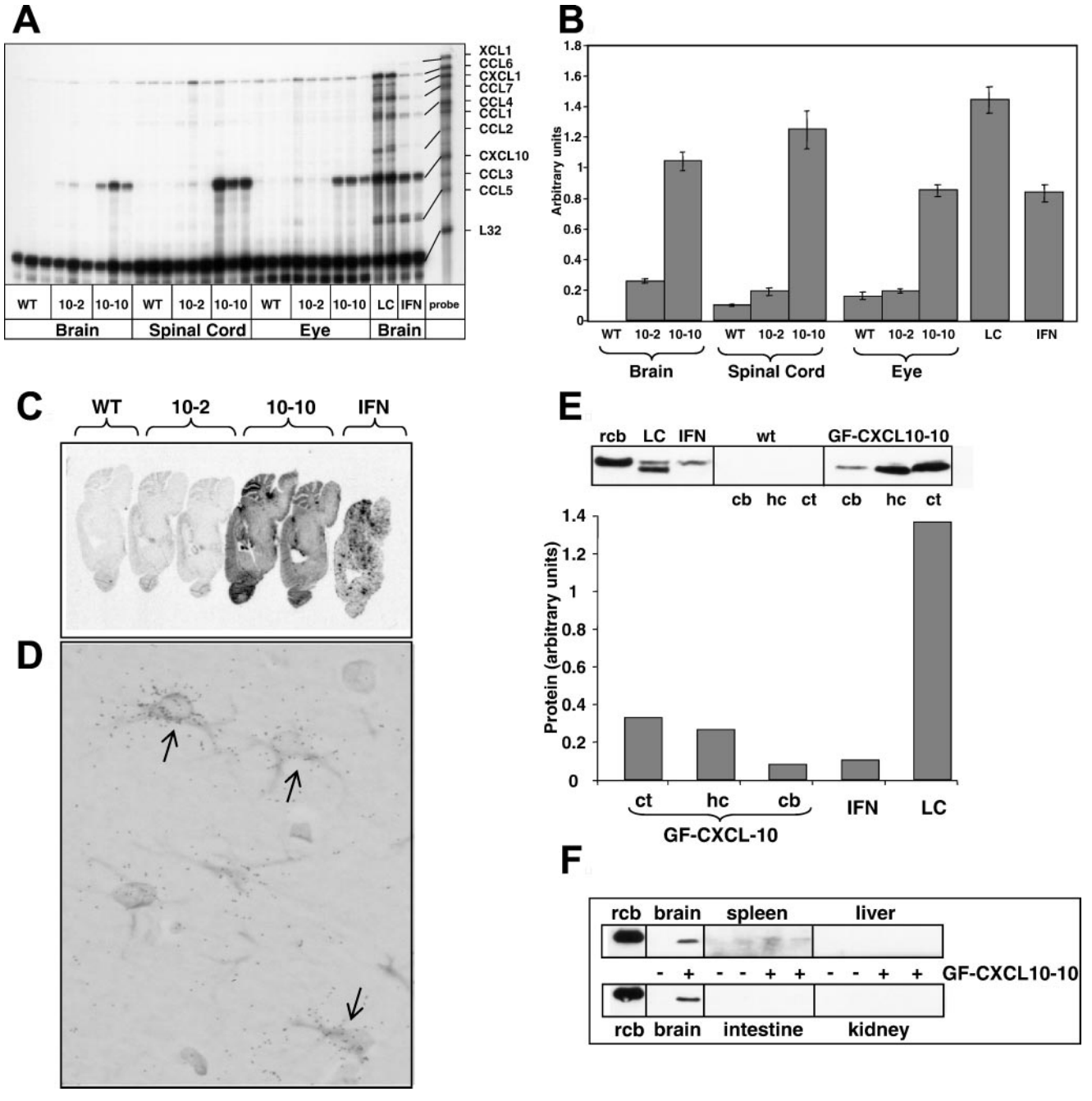

FIGURE 1. Analysis of CXCL10 RNA and protein expression in GF-CXCL10 transgenic mice. *A*, Chemokine mRNA expression was detected by RPA using a multiprobe set as described in *Materials and Methods*. For the RPA, 1 μg of poly(A)$^+$ RNA for brain samples and 10 μg of total RNA for spinal cord and eye samples were analyzed. Brains examined were from wild-type (WT), GF-CXCL10-2 (10-2), and GF-CXCL10-10 (10-10) mice. In addition, brain from mice infected with LCMV (LC) at 6 days postinfection and GFAP-IFNα (IFN) transgenic mice were included as positive controls. All animals used for this experiment were between 2 and 3 mo of age. *B*, Quantitative gene expression analysis. The autoradiograph in *A* was scanned and subjected to densitometry analysis using NIH 1.57 software. Bands were normalized to the ribosomal *rpl32* gene, which served as an internal loading control. Error bars represent SEM; $n = 3$. *C*, Anatomical localization of CXCL10 gene expression analyzed by in situ hybridization. The brain of mice (between 5 and 8 mo of age) from the various genotypes shown was removed, processed, and analyzed using a 726-bp antisense probe for the murine CXCL10 gene as described in *Materials and Methods*. Images are from autoradiography after a 4-day exposure. *D*, Cellular localization of CXCL10 gene expression in GF-CXCL10-10 transgenic mice. Sections were dual-labeled by in situ hybridization to detect CXCL10 RNA followed by immunohistochemistry with an anti-GFAP Ab to identify astrocytes as described in *Materials and Methods*. Colocalization of CXCL10 mRNA and GFAP protein is shown for astrocytes (arrows). Original magnification: $\times$600. *E*, Determination of CXCL10 protein levels in the brain. *Upper panel*, Immunoblot analysis of CXCL10 expression in cortex (ct), hippocampus (hc), and cerebellum (cb) of GF-CXCL10-10 and wild-type mice, respectively. Cerebellum from a GF-IFNα (IFN) mouse, olfactory bulb from a LCMV (LC)-infected wild-type mouse 6 day postinfection, and recombinant CXCL10 (rcb) protein were included as positive controls. A total of 400 μg of protein for each brain sample or 75 μg of the LCMV-infected olfactory bulb were analyzed. *Lower panel*, Quantitative protein expression analysis. Individual bands were scanned and quantitated using NIH 1.57 software. All bands were normalized to the relative amount of protein loaded for each lane. *F*, Comparison of CXCL10 protein expression in different organs. Tissue lysates were prepared and 400 μg of each was used for immunoblot analysis as described in *Materials and Methods*.

and transgenic mice with astrocyte-targeted production of IFN-α in the CNS (Fig. 1, *A* and *B*), suggesting that the level of CXCL10 mRNA in the GF-CXCL10-10 mice was within pathophysiologically relevant levels.

The spatial pattern of transgene-encoded CXCL10 RNA expression was determined by in situ hybridization. Autoradiographic analysis of the hybridized sections revealed background hybridization in wild-type brain. Consistent with our findings by RPA, CXCL10 RNA levels were found to be low in mice from the GF-CXCL10-2 line and markedly higher in the GF-CXCL10-10 line (Fig. 1*C*). Areas with the highest CXCL10 RNA were the olfactory bulb, hippocampal region, periventricular zone, cortical areas, cerebellum, and choroid plexus. Dual label analysis using an anti-GFAP Ab to specifically stain astrocytes served to identify the cellular source of CXCL10 gene expression and revealed numerous double-positive cells in animals of the GF-CXCL10-10 line (Fig. 1*D*). Thus, transgene-encoded CXCL10 gene expression was mediated by astrocytes distributed widely throughout the CNS.

To confirm that the GFAP-CXCL10 transgene also directed CXCL10 protein production, immunoblot analysis was performed. The presence of a protein species with similar size to recombinant murine CXCL10 was observed in cortex, hippocampus, and cerebellum from GF-CXCL10-10 transgenic but not wild-type mice (Fig. 1*E*). The level of CXCL10, which was higher in the cortex and hippocampus than in the cerebellum of the GF-CXCL10 brain, was also higher than in whole brain from GF-IFNα transgenic mice but was lower than in the olfactory bulb of mice with LCMV infection. A comparison of different organs from GF-CXCL10-10 and wild-type mice showed no significant differences between the two groups, with low or no detectable CXCL10 in spleen or other peripheral organs, respectively (Fig. 1*F*). In all, these findings confirm the CNS-specific production of CXCL10 protein in the GF-CXCL10 mice.

Spontaneous leukocyte infiltration in the CNS of GF-CXCL10 transgenic mice in the absence of altered expression levels of various inflammation-related genes

Routine histologic analysis of H&E-stained paraffin sections was used to examine for possible pathological alterations in the CNS of the GF-CXCL10 transgenic mice of different ages (2–8 mo). Compared with control littermates (Fig. 2, *A* and *B*), brain from GF-CXCL10 transgenic mice showed transgene dose- and age-dependent inflammatory lesions consisting of leukocyte infiltrates in forebrain and hindbrain areas. The size and number of these lesions was greatest in older animals of the GF-CXCL10-10 line and were most prominent in perivascular, meningeal, and ventricular regions of the brain (Fig. 2, *D* and *E*; arrows). In contrast, only minor leukocyte infiltration was evident in the brain of similarly aged mice of the GF-CXCL10-2 line (Fig. 2*C*; arrows). Peripheral organs including the kidney, liver, and skeletal muscle appeared normal in aged mice from both transgenic lines (data not shown). Further examination of the composition of the leukocyte infiltrates in the brain of GF-CXCL10-10 mice revealed, surprisingly, that a considerable number of neutrophils were present (Fig. 2*F*; arrows), while there were lower numbers of mononuclear cells (Fig. 2*F*; arrowheads). Other than leukocyte infiltration, there were no discernible pathologic alterations in the brain of GF-CXCL10 mice of either transgenic line at any age studied (up to 12 mo). In addition, immunostaining for GFAP in these brain sections revealed no observable differences between wild-type and GF-CXCL10-10 brains (data not shown). Because astrocytes are known to react to CNS injury or inflammation with increased GFAP production, this finding is consistent with the H&E stains in indicating that, despite leukocyte infiltration and accumulation, there was an absence of degenerative pathology in the brain of the GF-CXCL10 transgenic mice.

To clarify further the cellular composition of the leukocytic infiltrates in the brain of GF-CXCL10-10 mice, immunohistochemical analysis was performed (Fig. 3). Staining with the pan-leukocyte marker CD45 (Fig. 3, *A* and *B*) confirmed the presence of leukocyte infiltrates in the CNS of GF-CXCL10-10 transgenic mice (Fig. 3*B*), while in wild-type control mice (Fig. 3*A*) CD45 staining was restricted to perivascular microglia. Lower numbers of the infiltrating leukocytes were lymphocytes, with most of these being CD4-positive T cells (Fig. 3*D*), while CD8-positive cells were rare (data not shown). A significant number of the infiltrating leukocytes in the brain of the transgenic mice were positive for the neutrophil marker 7/4 (Fig. 3*F*). Cells bearing the granulocyte marker Gr1 (Fig. 3*H*) and the monocyte/macrophage marker

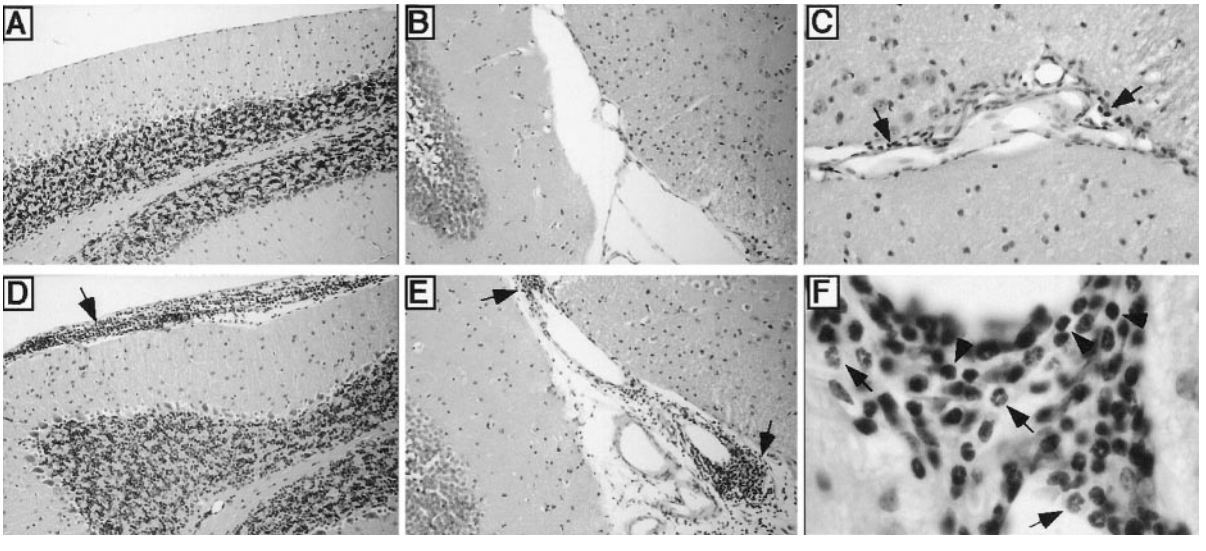

FIGURE 2. Leukocyte infiltration in the brain of GF-CXCL10 mice. H&E stains showing normal morphology of both cerebellum (*A*) and lateral ventricle region (*B*) in a wild-type mouse. In contrast, leukocyte infiltrates (arrows) were found in many areas in GF-CXCL10-10 transgenic mice, including as shown here in cerebellar meninges (*D*; arrow) and around vessels in the lateral ventricle (*E*; arrows). Only small numbers of leukocytes were evident in the brain from GF-CXCL10-2 mice (*C*; arrows). Original magnifications: ×200 for *A*, *B*, *D*, and *E*; ×400 for *C*. At a higher magnification (*F*, ×600), the presence of many neutrophils (arrows) and lesser numbers of mononuclear cells (arrowheads) could be seen within the leukocyte infiltrates.

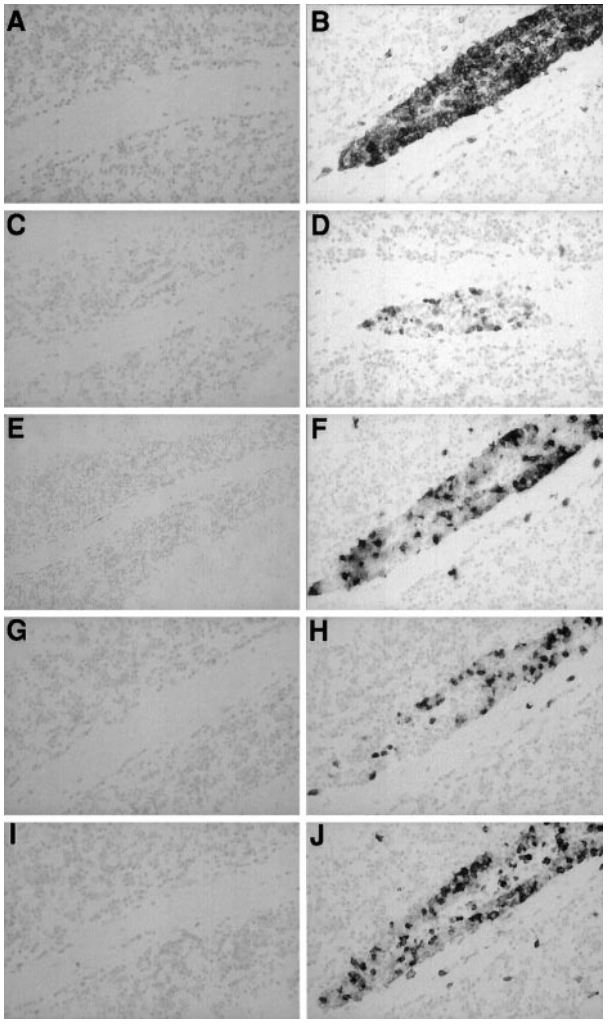

FIGURE 3. Immunophenotypic characterization of infiltrating leukocytes in brain of GF-CXCL10 mice. Immunohistochemistry was performed as described in *Materials and Methods* on cryosections of brain from wild-type (*A*, *C*, *E*, *G*, and *I*) and GF-CXCL10-10 (*B*, *D*, *F*, *H*, and *J*) mice. Sections were immunostained for CD45 (*A* and *B*), CD4 (*C* and *D*), 7/4 (*E* and *F*), Gr1 (*G* and *H*), and Mac-1 (*I* and *J*). Original magnification for all panels: ×400.

Mac-1 (Fig. 3*J*) were also prevalent. In general, the extent of leukocyte infiltration was higher in brain than in spinal cord of the GF-CXCL10-10 mice, with no significant differences in the cellular composition of the infiltrates (data not shown).

We next determined whether the expression of a variety of inflammation-related genes might be altered in the brain of GF-CXCL10-10 mice. As shown in Fig. 1, with the exception of the transgene-encoded CXCL10, cerebral expression of a large number of other chemokine genes was not detectable or altered in GF-CXCL10 mice, similar in this respect to the wild-type controls. A second chemokine probe set was used which included probes against a variety of additional chemokines (Table I), and this revealed no significant differences in gene expression levels between CXCL10 mice and wild-type littermates (data not shown). In addition to the chemokines, the expression of a large number of genes corresponding to the proinflammatory (e.g., IFN-γ, IFN-β, IL-1β, IL-4, IL-6, IL-12p40, and TNF) and counterinflammatory (e.g., TGF-β and IL-10) cytokines, MMPs (e.g., MMP2, 3, 9, and 12), TIMPs (e.g., TIMP-1), and antiviral response (e.g., RNA-dependent protein kinase R and 2′5′oligoadenylate synthetase) was not altered in the brain of CXCL10 mice compared with wild-type controls (data not shown). Taken together, these findings indicated that, while leukocyte infiltrates developed in the CNS of the GF-CXCL10 transgenic mice, this was not associated with an activated immune process.

Leukocyte recruitment to the brain of GF-CXCL10 transgenic mice is enhanced following peripheral immune challenge

Because CXCL10 and its receptor are linked to leukocyte trafficking in activated immune responses, we subjected young (2-mo-old) GF-CXCL10-10 mice and wild-type littermates to peripheral immune challenge by immunizing with CFA/PTX—a strategy known to activate type I immunity (63). As evidenced by staining for the pan-leukocyte marker CD45 (Fig. 4), in young nonimmunized GF-CXCL10 mice, compared with wild-type mice, only minor leukocyte infiltration was evident in some (two of three) animals. However, following immunization with CFA/PTX, GF-CXCL10-10 mice showed large accumulations of $CD45^+$ cells in perivascular, meningeal, and ventricular regions of the forebrain and hindbrain. This response peaked around days 8–14. Few $CD45^+$ cells were seen in CFA/PTX-immunized wild-type mice (Fig. 4). Additional phenotypic analysis of the infiltrating leukocytes in the brain of CFA-immunized GF-CXCL10-10 mice revealed these to be predominantly neutrophils (7/4) and monocyte/macrophages (Mac-1), with lesser numbers of $CD4^+$ and $CD8^+$ T cells (Fig. 4). These findings indicated that astrocyte production of CXCL10 markedly enhanced the recruitment of leukocytes to the brain following peripheral immune stimulation. Furthermore, similar to the lesions that developed spontaneously in the GF-CXCL10 mice following

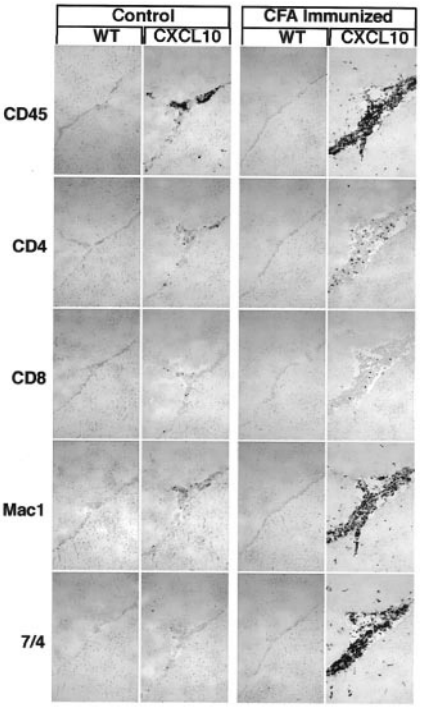

FIGURE 4. Leukocyte infiltration of the brain is increased in GF-CXCL10 mice following a peripheral immune challenge. Mice were actively immunized with CFA/PTX as described in *Materials and Methods*. At day 8 brains from nonimmunized or immunized wild-type and GF-CXCL10 mice were analyzed by immunohistochemistry performed as described in *Materials and Methods*. Sections were immunostained for the determinants shown here and described in *Materials and Methods*. Original magnification for all panels: ×400.

immune challenge in these animals, the majority of lesion-containing cells were neutrophils and monocyte/macrophages with lesser numbers of T cells.

We next determined (Fig. 5) whether there was altered immune accessory molecule (MHC class II, ICAM-1, VCAM-1) and extracellular matrix (ECM; fibronectin) deposition in the CNS of nonimmunized and immunized GF-CXCL10-10 mice. MHC class II and ICAM-1 were elevated on infiltrating leukocytes in GF-CXCL10-10 mice and this was increased further by CFA immunization. However, parenchymal cells as well as the vascular endothelium did not show any significant alterations in the expression of these molecules. Expression of VCAM-1 was limited to the vascular endothelium and was only increased in immunized GF-CXCL10-10 mice. Finally, the ECM molecule fibronectin is a component of the basement membrane and provides a useful marker not only for this structure but also for general vascular morphology and density. Fibronectin levels were elevated in the GF-CXCL10 mice in both lesion-associated and non-lesion-associated areas of the brain, and this increased further following CFA immunization. While this indicated an increase in the thickness of the basement membrane, the overall density and structure of the blood vessels appeared normal.

We next examined whether the increased leukocyte recruitment in CFA/PTX-immunized GF-CXCL10 transgenic mice was associated with alterations in gene expression levels of a number of cytokines or chemokines as determined by RPA (Fig. 6). In nonimmunized (day 0) and immunized wild-type mice, there was little detectable expression of any cytokine or chemokine gene examined. By contrast, the marked increase in leukocyte infiltration in immunized GF-CXCL10 transgenic mice was also accompanied by transient up-regulation in the expression of some chemokines (e.g., CCL6 and CCL2) and cytokines (e.g., TNF, IL-1α, and IL-1β). This response peaked around days 8–14 postimmunization before returning to undetectable levels by day 28.

CD3-positive but not Gr1-positive cells coexpress CXCR3 in the brain of GF-CXCL10 mice

The finding that a high number of leukocytes recruited to the brain of the GF-CXCL10 mice either spontaneously or following CFA/PTX immune stimulation were neutrophils was surprising, because

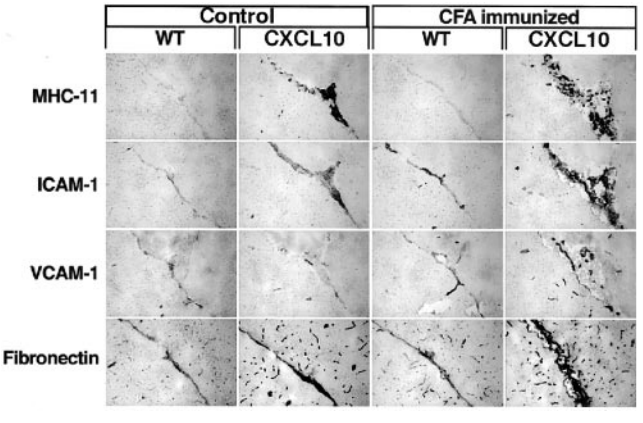

FIGURE 5. Increased expression of immune accessory molecules in the brain from GF-CXCL10-10 mice following a peripheral immune challenge. Mice were actively immunized with CFA/PTX as described in *Materials and Methods*. At day 8 brains from nonimmunized or immunized wild-type and GF-CXCL10 mice were analyzed by immunohistochemistry performed as described in *Materials and Methods*. Sections were immunostained for the determinants as shown here and described in *Materials and Methods*. Original magnification for all panels: ×400.

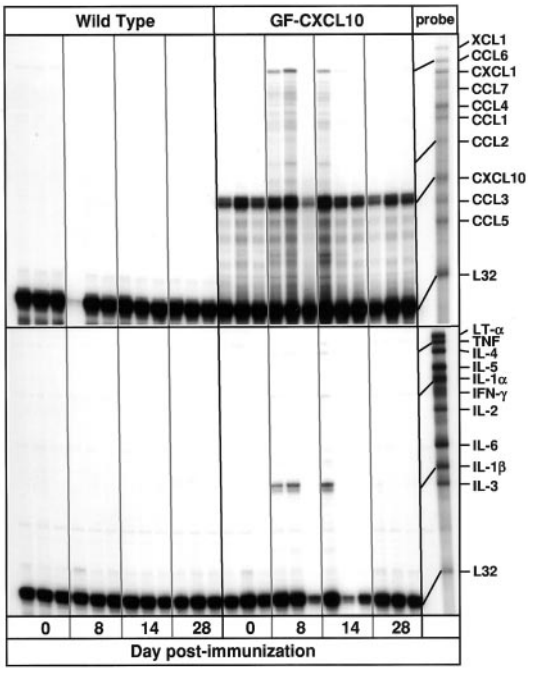

FIGURE 6. The expression of some chemokine (*upper panel*) and cytokine (*lower panel*) genes was transiently increased in the brain of GF-CXCL10-10 mice following a peripheral immune challenge. Mice were actively immunized with CFA/PTX as described in *Materials and Methods*. At the days shown, brains from nonimmunized or immunized wild-type and GF-CXCL10 mice were removed and poly(A)$^+$ RNA was isolated as described in *Materials and Methods*. For chemokine and cytokine gene expression, 1 μg of RNA was analyzed by RPA as described in *Materials and Methods*.

these cells have previously been shown not to exhibit a chemotactic response to CXCL10 in vitro (4, 64). Therefore, we wished to define further the expression of the CXCL10 receptor CXCR3 in the CNS and on the predominant infiltrating leukocyte populations.

By both RPA (Fig. 7*A*) and immunoblot (Fig. 7*B*) analysis, we were able to readily detect CXCR3 RNA and protein in spleen but not in brain from wild-type mice. To derive enough cells to examine the levels of CXCR3 expression on the infiltrating leukocytes in the brain of the GF-CXCL10 mice, it was necessary to first challenge these animals with CFA/PTX. In spleen cell suspensions from naive mice, ~13% of the gated cells were CXCR3 positive (Fig. 7, *F*, *I*, and *L*). Of these, the majority (~90%) coexpressed the T cell marker CD3 (Fig. 7*L*), while only a minority (≤10%) of the spleen cells coexpressed the CXCR3 and 7/4 (Fig. 7*F*) or Gr1 (Fig. 7*I*) markers. The overall numbers of CXCR3-positive cells did not change markedly in spleen from mice that had been immunized with CFA/PTX (Fig. 7, *G*, *J*, and *M*), nor did the relative numbers coexpressing the CXCR3 and CD3 (Fig. 7*M*) or Gr1 (Fig. 7*J*) markers. However, the fraction of cells coexpressing CXCR3 and 7/4 increased to 30% (Fig. 7*G*). It should be noted that there was a large increase in the overall number of 7/4- and Gr1-positive cells in spleen cell suspensions from CFA/PTX-immunized (Fig. 7, *G* and *J*) compared with naive (Fig. 7, *F* and *I*) mice.

As noted above, some 13% of splenocytes both from naive and CFA/PTX-immunized mice express CXCR3. A parallel analysis of leukocytes isolated from the brain of CFA/PTX-immunized GF-CXCL10-10 mice revealed a selective accumulation of CXCR3-positive cells in this tissue, which represented ~30% of the gated cells (Fig. 7, *H*, *K*, and *N*). Further analysis of the CNS-infiltrating leukocyte population revealed that selective enrichment for

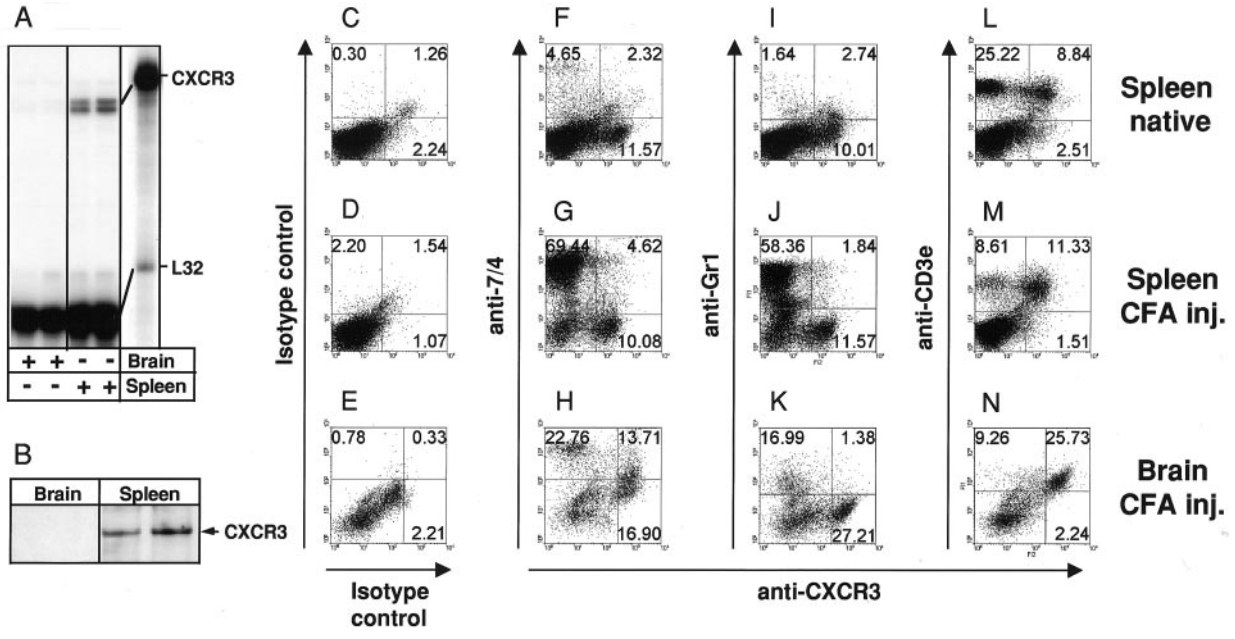

FIGURE 7. CXCR3 RNA or protein was detectable in immune but not CNS tissues and cells. CXCR3 expression was analyzed by RPA (*A*), immunoblot (*B*), or FACS (*C–N*). For RPA, poly(A)$^+$ RNA was isolated from the spleen or brain of wild-type mice and 2.5 μg was used for RPA as described in *Materials and Methods*. Immunoblot analysis of CXCR3 protein was done on spleen and brain protein lysates from wild-type mice. Protein samples were prepared and analyzed as described in *Materials and Methods*. For flow cytometric analysis of CXCR3 surface expression, different leukocyte subsets were isolated from spleen of wild-type mice or spleen and brain from GF-CXCL10-10 transgenic mice 10 days after CFA/PTX immunization. Leukocyte single-cell suspensions were prepared as described in *Materials and Methods* and surface stained for the neutrophil marker 7/4, the granulocyte marker Gr1, or the T cell marker CD3 and their respective, isotype-matched control Abs. Dual labeling using anti-murine CXCR3 Ab served to correlate CXCR3 expression with the various leukocyte subsets (*F–N*). *C–E*, Results obtained with the various isotype-matched control Abs for each of the markers used. A total of 50,000 and 20,000 events for splenic leukocytes and the Percoll gradient prepared from brain, respectively, were gated on leukocytes and analyzed using WinMDI 2.8 software. The numbers in each quadrant indicate the respective percentage of gated events. The data demonstrate that there is selective enrichment for CXCR3-positive cells in the brain of CFA/PTX-immunized GF-CXCL10-10 transgenic mice (*H*, *K*, and *N*), as compared with spleen single-cell suspensions (*G*, *J*, and *M*). While almost the entire population of cells positive for CXCR3 coexpressed CD3 (*N*), cells positive for the granulocyte marker Gr1 were negative for CXCR3 expression (*I*). Note also how peripheral immunization with CFA/PTX leads to drastic increase in the number of 7/4- and Gr1-positive cells in the spleen (*G* and *J*) as compared with native spleen cells (*F* and *I*).

CXCR3-positive cells was also represented by the 7/4 (Fig. 7*H*) and CD3 (Fig. 7*N*), but not Gr1, cell populations. In fact, almost 50% of the CXCR3-positive cells coexpressed the 7/4 marker (Fig. 7*H*), while 100% coexpressed CD3. In contrast, few if any Gr1-positive cells were also CXCR3 positive (Fig. 7*K*).

Discussion

The IFN-inducible non-ELR chemokine CXCL10 is implicated in the pathogenesis of a wide spectrum of neurological disorders. The present study was aimed at better understanding the CNS actions of this chemokine by developing transgenic mice with astrocyte-targeted expression of the CXCL10 gene. This approach has been used by us previously to investigate the function of number of proinflammatory cytokines (reviewed in Ref. 65). Our results showed that, similar to cytokines such as TNF (51) and IL-12 (56), the chronic astrocyte production of CXCL10 is sufficient to initiate and maintain the infiltration of leukocytes to the CNS in otherwise unmanipulated mice and to markedly enhance CNS leukocyte infiltration after nonspecific peripheral immune challenge. However, in contrast to the proinflammatory cytokines, and despite the presence of prominent leukocyte infiltration affecting various brain regions, these cells were apparently not involved in an active inflammatory process leading to CNS tissue destruction. Consistent with this, the transgenic animals did not show any behavioral or physical abnormalities. No other significant molecular or cellular neuropathological alterations were found in the brain of the unmanipulated GF-CXCL10 mice compared with wild-type control littermates. Therefore, these findings suggested that 1) CXCL10 produces little if any direct effects in the normal CNS, and 2) under pathological conditions, while CXCL10 recruits leukocytes into the CNS, additional factors including proinflammatory cytokines are likely necessary to mediate full activation of their effector functions.

Our findings here for the CNS production of CXCL10 contrast with the situation in skin with transgenic production of this chemokine. Thus, chronic production of CXCL10 by keratinocytes in the skin did not promote spontaneous recruitment of leukocytes (66). In addition, these transgenic mice had normal cutaneous contact hypersensitivity cellular immune responses, suggesting that CXCL10 did not influence the development of a T cell-dependent immune response induced in the skin. Differences between the skin vs pancreas for the recruitment of T cells or monocytes has been described previously for the transgenic production in these tissues of CCL21 (67) or monocyte chemoattractant protein-1 (68, 69), respectively. In all, these findings suggest that transgene-driven production of chemokines in the skin does not always give rise to the expected leukocyte recruitment signature. The basis for this phenomenon is not known but could reflect the involvement of additional tissue-specific factors in mice that might interact with a given chemokine to influence its chemoattractant potential and specificity.

Transgenic expression of a number of chemokine genes in the CNS has been accomplished previously using the myelin basic protein promoter to drive oligodendrocyte production of CCL2

(70), CXCL1 (71), CCL19, and CCL21 (72). In this regard, CXCL10 is similar to CCL2 or CXCL1, with production of the latter by oligodendrocytes stimulating leukocyte recruitment to the CNS, but not activation or destructive immune pathology in the CNS. By contrast, the oligodendrocyte production of CCL21 induced CNS inflammation with infiltration by neutrophils and eosinophils in association with neurological disease characterized by reactive gliosis, demyelination, motor impairment, and premature death (72). However, whether the neurological disease in this setting was directly related to an inflammatory process mediated by the infiltrating neutrophils and eosinophils was not established.

In the context of the present studies, it was of interest that there was a lack of parenchymal penetration by the CXCR3-expressing T cells, even though parenchymal cells produced CXCL10. It is unclear at the present time why this was the case. Many explanations are possible, including the inability to establish an effective CXCL10 gradient in the parenchyma due to the diffuse chronic production of the chemokine throughout the brain astrocyte population. An additional possibility may include the presence of molecules that inhibit or modify the further migration of the T cells. In this context, it is of interest to note that the nature of the ECM can play an important role in regulating the behavior and extravascular migration of leukocytes (73). We have found in the present report that changes in the ECM, as indicated by increased fibronectin deposition, were indeed apparent. However, whether and to what extent such modification of the ECM under these circumstances influenced parenchymal T cell migration remains to be determined.

A somewhat surprising finding from our study was the nature of the inflammatory infiltrates present in the brain of the GF-CXCL10 transgenic mice. CXCL10 is classically known to induce chemotaxis of activated CD4-positive Th1 and CD8 T cells, NK cells, and cells of the monocyte/macrophage population (4, 6, 74), but has been reported not to effect human neutrophil chemotaxis (64). Consistent with this, in the experimental models of T cell-mediated neurological disease (EAE (43) and MHV encephalomyelitis (45)) Ab neutralization of CXCL10 is associated with a dramatic reduction in the CNS infiltration of T cells and macrophages. Yet, in GF-CXCL10 transgenic mice, a significant number of the infiltrating leukocytes were neutrophils, as assessed by H&E staining as well as by immunohistochemistry using mAb against the neutrophil marker 7/4 and the granulocyte marker Gr1 (75, 76). CXCL10 has been shown to act preferentially on activated rather than resting human T cells (4, 6); this correlated with the presence of the CXCL10 receptor CXCR3 on activated but not resting T cells (6). Based on this information, it is not surprising that T cells may comprise only a minority of cells in the spontaneous inflammatory lesions of unmanipulated mice. However, even following peripheral immune activation with CFA/PTX immunization, a strategy known to induce a strong type I immune response with activation of Th1 cells (63, 77), the inflammatory lesions in the brain of the GF-CXCL10 mice were dominated by neutrophils with much smaller numbers of CD4 and CD8 T cells present. The dominant presence of neutrophils in the GF-CXCL10 mice could not be explained by the increased expression in the brain of other cytokines or chemokines, such as CXCL1, that are known to stimulate neutrophil chemotaxis (78). Thus, we conclude from these findings that, in vivo, CXCL10 on its own is an effective chemoattractant for neutrophils to the brain. The notion that CXCL10 can act on neutrophil trafficking in vivo is further supported by a recent report showing that this chemokine plays a primary role in neutrophil recruitment in a murine model of oxidative stress-induced lung inflammation (79). Human neutrophils can produce CXCL10 (80), raising the possibility that CXCL10 might function as an autocrine factor for these cells.

As one approach to address the possible mechanisms underlying the nature of the leukocytes that are attracted to the CNS of GF-CXCL10 mice, we analyzed the expression of the CXCL10 receptor CXCR3 on neutrophils and T cells in spleen single-cell suspensions and in leukocytes isolated from the brain of CFA/PTX-stimulated GF-CXCL10 mice. In spleen single-cell suspensions from both nonimmunized and immunized GF-CXCL10 transgenic mice, similar overall numbers of cells were found to be positive for expression of the receptor CXCR3. This suggested that immunization with CFA/PTX did not alter the total number of CXCR3-positive cells or that it may have up-regulated CXCR3 expression on leukocytes, but these subsequently emigrated into the periphery, hence leaving the relative fraction of CXCR3-positive cells within the spleen unaltered. A further point raised by these findings is that an unexpectedly large number of splenic T cells from nonimmunized mice expressed CXCR3. This suggests that, at least in the mouse, T cell activation is not required for expression of CXCR3. Compared with the spleen, the CNS of CFA/PTX-immunized GF-CXCL10-10 transgenic mice was enriched significantly for CXCR3-positive cells. This observation is consistent with a directed chemotactic response mediated by the presence of CXCL10 in the brain. Detailed analysis of CXCR3 receptor expression on leukocytes recruited to the brain of the GF-CXCL10 transgenic mice revealed differences among the various subsets of leukocytes. Thus, a majority of T cells accounted for most of the CXCR3-expressing cells, while little if any expression of this molecule was detectable by cells positive for the granulocyte marker Gr1. Because neutrophils are also positive for Gr1, this suggested that these cells must be CXCR3 negative. However, a subset of cells positive for the neutrophil marker 7/4 were clearly positive for CXCR3. The apparent dichotomy here might be explained by the fact that the 7/4 marker (76), but not the Gr1 (81) marker, is also expressed at low levels on a subset of activated macrophages. In all, our findings suggest that the accumulation of neutrophils in the brain of GF-CXCL10 transgenic mice is independent of CXCR3 and therefore involves an as-yet-undefined mechanism. Such a mechanism might involve the expression of an alternative receptor for CXCL10 by neutrophils. In this context, evidence for an alternative functional CXCL10 receptor has come from studies of CXCR3-negative human epithelial and endothelial cells (21).

Besides leukocyte chemotaxis, CXCL10 displays other actions, including marked antiangiogenic activity (9–11). In the present study, the chronic astrocyte production of CXCL10 in the CNS did not produce any abnormal signs of dysgenesis or agenesis of the CNS vasculature. It should be noted that GFAP gene expression is present from E17 onwards, with maximum expression occurring around days 10–14 postnatally (82, 83)—a time at which brain angiogenesis is nearly complete. Similar to our finding here, Luster et al. (66) reported no developmental defects in skin vasculature in transgenic mice with keratinocyte-targeted expression of CXCL10. However, these mice displayed an abnormal wound healing response due to impaired blood vessel formation upon exogenous injuries. In preliminary studies (I. L. Campbell, unpublished observations), we have found marked suppression of cerebral angiogenesis in the CNS of transgenic mice bigenic for both astrocyte-targeted IL-6 and CXCL10 production. GF-IL-6 mice were shown previously to have a chronic proliferative angiopathy (49, 84). In total, these different studies suggest that physiological angiogenesis such as occurs during CNS development might not be markedly perturbed by the presence of CXCL10; however, this chemokine is capable of suppressing this process when it is induced under pathological conditions. Further work will be necessary to address in detail the effects of CXCL10 on angiogenesis in specific microenvironments such as the brain. It will also be important to determine whether a recently described alternative functional receptor for

CXCL10 that is expressed on endothelial cells (21) might contribute to the angiostatic effects of CXCL10.

In summary, we have developed a novel transgenic model for the chronic, astrocyte-targeted production of CXCL10. The findings indicated that 1) CXCL10 can promote spontaneous and potentiate immune-induced recruitment of leukocytes, particularly neutrophils, to the CNS; 2) CXCL10-induced leukocyte accumulation in the brain was not associated with activation of a degenerative immune pathology; and 3) the dominant accumulation of neutrophils in the brain of GF-CXCL10 transgenic mice occurred independent of CXCR3 and therefore through an as-yet-unidentified mechanism. The availability of the GF-CXCL10 mouse should now permit some of these outstanding issues to be studied and hopefully clarified.

Acknowledgments

We thank Heather Weinkauf and Mary Kies-Wagner for their technical support in the breeding, screening, and maintenance of the GF-CXCL10 mice and Dr. Daniel E. Hassett for his helpful advice with the flow cytometry experiments. We are grateful for the administrative support of Heather Kemlein.

References

1. Luster, A. D., J. C. Unkeless, and J. V. Ravetch. 1985. γ-Interferon transcriptionally regulates an early-response gene containing homology to platelet proteins. *Nature 315:672.*
2. Luster, A. D., and J. V. Ravetch. 1987. Biochemical characterization of a γ interferon-inducible cytokine (IP-10). *J. Exp. Med. 166:1084.*
3. Vanguri, P., and J. M. Farber. 1990. Identification of CRG-2: an interferon-inducible mRNA predicted to encode a murine monokine. *J. Biol. Chem. 265: 15049.*
4. Taub, D. D., A. R. Lloyd, K. Conlon, J. M. Wang, J. R. Ortaldo, A. Harada, K. Matsushima, D. J. Kelvin, and J. J. Oppenheim. 1993. Recombinant human-interferon-inducible protein 10 is a chemoattractant for human monocytes and T lymphocytes and promotes T cell adhesion to endothelial cells. *J. Exp. Med. 177:1809.*
5. Qin, S., J. B. Rottman, P. Myers, N. Kassam, M. Weinblatt, M. Loetscher, A. E. Koch, B. Moser, and C. R. Mackay. 1998. The chemokine receptors CXCR3 and CCR5 mark subsets of T cells associated with certain inflammatory reactions. *J. Clin. Invest. 101:746.*
6. Loetscher, M., B. Gerber, P. Loetscher, S. A. Jones, L. Piali, I. Clark Lewis, M. Baggiolini, and B. Moser. 1996. Chemokine receptor specific for IP10 and Mig: structure, function, and expression in activated T-lymphocytes. *J. Exp. Med. 184:963.*
7. Mahalingam, S., J. M. Farber, and G. Karupiah. 1999. The interferon-inducible chemokines MuMig and Crg-2 exhibit antiviral activity in vivo. *J. Virol. 73:1479.*
8. Cole, A. M., T. Ganz, A. M. Liese, M. D. Burdick, L. Liu, and R. M. Strieter. 2001. Cutting edge: IFN-inducible ELR^- CXC chemokines display defensin-like antimicrobial activity. *J. Immunol. 167:623.*
9. Angiolillo, A. L., C. Sgadari, D. D. Taub, F. Liao, J. M. Farber, S. Maheshwari, H. K. Kleinman, G. H. Reaman, and G. Tosato. 1995. Human interferon-inducible protein 10 is a potent inhibitor of angiogenesis in vivo. *J. Exp. Med. 182:155.*
10. Strieter, R. M., S. L. Kunkel, D. A. Arenberg, M. D. Burdick, and P. J. Polverini. 1995. Interferon γ-inducible protein 10 (IP-10), a member of the C-X-C chemokine family, is an inhibitor of angiogenesis. *Biochem. Biophys. Res. Commun. 210:51.*
11. Luster, A. D., S. M. Greenberg, and P. Leder. 1995. The IP-10 chemokine binds to a specific cell surface heparan sulfate site shared with platelet factor 4 and inhibits endothelial cell proliferation. *J. Exp. Med. 182:219.*
12. Sgadari, C., A. L. Angiolillo, B. W. Cherney, S. E. Pike, J. M. Farber, L. G. Koniaris, P. Vanguri, P. R. Burd, N. Sheikh, G. Gupta, et al. 1996. Interferon-inducible protein-10 identified as a mediator of tumor necrosis in vivo. *Proc. Natl. Acad. Sci. USA 93:13791.*
13. Sgadari, C., A. L. Angiolillo, and G. Tosato. 1996. Inhibition of angiogenesis by interleukin-12 is mediated by the interferon-inducible protein 10. *Blood 87:3877.*
14. Liao, F., R. L. Rabin, J. R. Yannelli, L. G. Koniaris, P. Vanguri, and J. M. Farber. 1995. Human Mig chemokine: biochemical and functional characterization. *J. Exp. Med. 182:1301.*
15. Cole, K. E., C. A. Strick, T. J. Paradis, K. T. Ogborne, M. Loetscher, R. P. Gladue, W. Lin, J. G. Boyd, B. Moser, D. E. Wood, et al. 1998. Interferon-inducible T cell α chemoattractant (I-TAC): a novel non-ELR CXC chemokine with potent activity on activated T cells through selective high affinity binding to CXCR3. *J. Exp. Med. 187:2009.*
16. Soto, H., W. Wang, R. M. Strieter, N. G. Copeland, D. J. Gilbert, N. A. Jenkins, J. Hedrick, and A. Zlotnik. 1998. The CC chemokine 6Ckine binds the CXC chemokine receptor CXCR3. *Proc. Natl. Acad. Sci. USA 95:8205.*
17. Jenh, C.-H., M. A. Cox, H. Kaminski, M. Zhang, H. Byrnes, J. Fine, D. Lundell, C.-C. Chou, S. K. Narula, and P. J. Zavodny. 1999. Cutting edge: species specificity of the CC chemokine 6Ckine signaling through the CXC chemokine receptor CXCR3: human 6Ckine is not a ligand for the human or mouse CXCR3 receptors. *J. Immunol. 162:3765.*
18. Bonecchi, R., G. Bianchi, P. P. Bordignon, D. D'Ambrosio, R. Lang, A. Borsatti, S. Sozzani, P. Allavena, P. A. Gray, A. Mantovani, and F. Sinigaglia. 1998. Differential expression of chemokine receptors and chemotactic responsiveness of type 1 T helper cells (Th1s) and Th2s. *J. Exp. Med. 187:129.*
19. Khan, I. A., J. A. Maclean, F. S. Lee, L. Casciotti, E. DeHaan, J. D. Schwartzman, and A. D. Luster. 2000. IP-10 is critical for effector T cell trafficking and host survival in *Toxoplasma gondii* infection. *Immunity 12:483.*
20. Hancock, W. W., B. Lu, W. Gao, V. Csizmadia, K. L. Faia, J. A. King, S. T. Smiley, M. Ling, N. P. Gerard, and C. Gerard. 2000. Requirement of the chemokine receptor CXCR3 for acute allograft rejection. *J. Exp. Med. 192:1515.*
21. Soejima, K., and B. J. Rollins. 2001. A functional IFN-γ-inducible protein-10/CXCL10-specific receptor expressed by epithelial and endothelial cells that is neither CXCR3 nor glycosaminoglycan. *J. Immunol. 167:6576.*
22. Xia, M. Q., B. J. Baeski, R. B. Knowles, S. X. Qin, and B. T. Hyman. 2000. Expression of the chemokine receptor CXCR3 on neurons and the elevated expression of its ligand IP-10 in reactive astrocytes: in vitro ERK1/2 activation and role in Alzheimer's disease. *J. Neuroimmunol. 108:227.*
23. Sorensen, T. L., M. Tani, J. Jensen, V. Pierce, C. Lucchinetti, V. A. Folcik, S. Qin, J. Rottman, F. Sellebjerg, R. M. Strieter, et al. 1999. Expression of specific chemokines and chemokine receptors in the central nervous system of multiple sclerosis patients. *J. Clin. Invest. 103:807.*
24. Balashov, K. E., J. B. Rottman, H. L. Weiner, and W. W. Hancock. 1999. $CCR5^+$ and $CXCR3^+$ T cells are increased in multiple sclerosis and their ligands MIP-1α and IP-10 are expressed in demyelinating brain lesions. *Proc. Natl. Acad. Sci. USA 96:6873.*
25. Kolb, S. A., B. Sporer, F. Lahrtz, U. Koedel, H.-W. Pfister, and A. Fontana. 1999. Identification of a T cell chemotactic factor in the cerebrospinal fluid of HIV-1 infected individuals as interferon-γ inducible protein 10. *J. Neuroimmunol. 93: 172.*
26. Sanders, V. J., C. A. Pittman, M. G. White, G. Wang, C. A. Wiley, and C. L. Achim. 1998. Chemokines and receptors in HIV encephalitis. *AIDS 12: 1021.*
27. Lahrtz, F., L. Piali, D. Nadal, H. W. Pfister, K. S. Spanaus, M. Baggiolini, and A. Fontana. 1997. Chemotactic activity on mononuclear cells in the cerebrospinal fluid of patients with viral meningitis is mediated by interferon-γ inducible protein-10 and monocyte chemotactic protein-1. *Eur. J. Immunol. 27:2484.*
28. Glabinski, A. R., M. Tani, R. M. Strieter, V. K. Tuohy, and R. M. Ransohoff. 1997. Synchronous synthesis of α- and β-chemokines by cells of diverse lineage in the central nervous system of mice with relapses of chronic experimental autoimmune encephalomyelitis. *Am. J. Pathol. 150:617.*
29. Ransohoff, R. M., T. A. Hamilton, M. Tani, M. H. Stoler, H. E. Shick, J. A. Major, M. L. Estes, D. M. Thomas, and V. K. Tuohy. 1993. Astrocyte expression of mRNA encoding cytokines IP-10 and JE/MCP-1 in experimental autoimmune encephalomyelitis. *FASEB J. 7:592.*
30. Godiska, R., D. Chantry, G. N. Dietsch, and P. W. Gray. 1995. Chemokine expression in murine experimental allergic encephalomyelitis. *J. Neuroimmunol. 58:167.*
31. Asensio, V. C., S. Lassmann, A. Pagenstecher, S. C. Steffensen, S. J. Henriksen, and I. L. Campbell. 1999. C10 is a novel chemokine expressed in experimental inflammatory demyelinating disorders that promotes the recruitment of macrophages to the central nervous system. *Am. J. Pathol. 154:1181.*
32. Karpus, W. J., and R. M. Ransohoff. 1998. Chemokine regulation of experimental autoimmune encephalomyelitis: temporal and spatial expression patterns govern disease pathogenesis. *J. Immunol. 161:2667.*
33. Asensio, V. C., and I. L. Campbell. 1997. Chemokine gene expression in the brain of mice with lymphocytic choriomeningitis. *J. Virol. 71:7832.*
34. Asensio, V. C., C. Kincaid, and I. L. Campbell. 1999. Chemokines and the inflammatory response to viral infection in the central nervous system with a focus on lymphocytic choriomeningitis virus. *J. Neurovirol. 5:65.*
35. Lane, T. E., V. C. Asensio, N. Yu, A. D. Paoletti, I. L. Campbell, and T. E. Buchmeier. 1998. Dynamic regulation of α- and β-chemokine expression in the central nervous system during mouse hepatitis virus-induced demyelinating disease. *J. Immunol. 160:970.*
36. Theil, D. J., I. Tsunoda, J. E. Libbey, T. J. Derfuss, and R. S. Fujinami. 2000. Alterations in cytokine but not chemokine mRNA expression during three distinct Theiler's virus infections. *J. Neuroimmunol. 104:22.*
37. Murray, P. D., K. Krivacic, A. Chernosky, T. Wei, R. M. Ransohoff, and M. Rodriguez. 2000. Biphasic and regionally-restricted chemokine expression in the central nervous system in the Theiler's virus model of multiple sclerosis. *J. Neurovirol. 6:S44.*
38. McTigue, D. M., M. Tani, K. Krivacic, A. Chernosky, G. S. Kelner, D. Maciejewski, R. Maki, R. M. Ransohoff, and B. T. Stokes. 1998. Selective chemokine mRNA accumulation in the rat spinal cord after contusion injury. *J. Neurosci. 53:368.*
39. Wang, X., J. A. Ellison, A. L. Siren, P. G. Lysko, T. L. Yue, F. C. Barone, A. Shatzman, and G. Z. Feuerstein. 1998. Prolonged expression of interferon-inducible protein-10 in ischemic cortex after permanent occlusion of the middle cerebral artery in rat. *J. Neurochem. 71:1194.*
40. Bruccoleri, A., and G. J. Harry. 2000. Chemical-induced hippocampal neurodegeneration and elevations in TNFα, TNFβ, IL-1α, IP-10, and MCP-1 mRNA in osteopetrotic (*op*/*op*) mice. *J. Neurosci. Res. 62:146.*
41. Asensio, V. S., J. Maier, R. Milner, K. Boztug, C. Kincaid, M. Moulard, C. Phillipson, K. Lindsley, T. Krucker, H. S. Fox, and I. L. Campbell. 2001.

Interferon-independent, human immunodeficiency virus-1-gp120-mediated induction of CXCL10/IP-10 gene expression by astrocytes in vivo and in vitro. *J. Virol. 75:7067.*
42. Riemer, C., I. Queck, D. Simon, R. Kurth, and M. Baier. 2000. Identification of upregulated genes in scrapie-infected brain tissue. *J. Virol. 74:10245.*
43. Fife, B. T., K. J. Kennedy, M. C. Paniagua, N. W. Lukacs, S. L. Kunkel, A. D. Luster, and W. J. Karpus. 2001. CXCL10 (IFN-γ-inducible protein-10) control of encephalitogenic $CD4^+$ T cell accumulation in the central nervous system during experimental autoimmune encephalomyelitis. *J. Immunol. 166: 7617.*
44. Liu, M. T., H. S. Keirstead, and T. E. Lane. 2001. Neutralization of the chemokine CXCL10 reduces inflammatory call invasion and demyelination and improves neurological function in a viral model of multiple sclerosis[1]. *J. Immunol. 167:4091.*
45. Liu, M. T., B. P. Chen, P. Oertel, M. J. Buchmeier, D. Armstrong, T. A. Hamilton, and T. E. Lane. 2000. Cutting edge: the T cell chemoattractant IFN-inducible protein 10 is essential in host defense against viral-induced neurologic disease. *J. Immunol. 165:2327.*
46. Liu, M. T., D. Armstrong, T. A. Hamilton, and T. E. Lane. 2001. Expression of Mig (monokine induced by interferon-γ) is important in T lymphocyte recruitment and host defense following viral infection of the central nervous system. *J. Immunol. 166:1790.*
47. Campbell, I. L., A. K. Stalder, Y. Akwa, A. Pagenstecher, and V. C. Asensio. 1998. Transgenic models to study the actions of cytokines in the central nervous system. *Neuroimmunomodulation 5:126.*
48. Campbell, I. L., and C.-S. Chiang. 1995. Cytokine involvement in CNS disease: implications from transgenic mice. *Ann. NY Acad. Sci. 771:301.*
49. Campbell, I. L., C. R. Abraham, E. Masliah, P. Kemper, J. D. Inglis, M. B. A. Oldstone, and L. Mucke. 1993. Neurologic disease induced in transgenic mice by the cerebral overexpression of interleukin 6. *Proc. Natl. Acad. Sci. USA 90:10061.*
50. Chiang, C.-S., H. C. Powell, L. Gold, A. Samimi, and I. L. Campbell. 1996. Macrophage/microglial-mediated primary demyelination and motor disease induced by the central nervous system production of interleukin-3 in transgenic mice. *J. Clin. Invest. 97:1512.*
51. Stalder, A. K., M. J. Carson, A. Pagenstecher, V. C. Asensio, C. Kincaid, M. Benedict, H. C. Powell, E. Masliah, and I. L. Campbell. 1998. Late-onset chronic inflammatory encephalopathy in immune-competent and severe combined immune-deficient (SCID) mice with astrocyte-targeted expression of tumor necrosis factor. *Am. J. Pathol. 153:767.*
52. Akwa, Y., D. E. Hassett, M. L. Eloranta, K. Sandberg, E. Masliah, H. Powell, J. L. Whitton, F. E. Bloom, and I. L. Campbell. 1998. Transgenic expression of IFN-α in the central nervous system of mice protects against lethal neurotropic viral infection but induces inflammation and neurodegeneration. *J. Immunol. 161: 5016.*
53. Badley, J. E., G. A. Bishop, T. St. John, and J. A. Frelinger. 1988. A simple, rapid method for the purification of poly A^+ RNA. *BioTechniques 6:114.*
54. Stalder, A. K., and I. L. Campbell. 1994. Simultaneous analysis of multiple cytokine receptor mRNAs by RNase protection assay in LPS-induced endotoxemia. *Lymphokine Cytokine Res. 13:107.*
55. Hobbs, M. V., W. O. Weigle, D. J. Noonan, B. E. Torbett, R. J. McEvilly, R. J. Koch, G. J. Cardenas, and D. N. Ernst. 1992. Patterns of cytokine gene expression by $CD4^+$ T cells from young and old mice. *J. Immunol. 150:3602.*
56. Pagenstecher, A., S. Lassmann, M. J. Carson, C. L. Kincaid, A. K. Stalder, and I. L. Campbell. 2000. Astrocyte-targeted expression of IL-12 induces active cellular immune responses in the central nervous system and modulates experimental allergic encephalomyelitis. *J. Immunol. 164:4481.*
57. Pagenstecher, A., A. S. Stalder, and I. L. Campbell. 1997. RNase protection assays for the simultaneous and semiquantitative analysis of multiple murine matrix metalloproteinase (MMP) and MMP inhibitor mRNAs. *J. Immunol. Methods 206:1.*
58. Chiang, C.-S., A. Stalder, A. Samimi, and I. L. Campbell. 1994. Reactive gliosis as a consequence of interleukin-6 expression in the brain: studies in transgenic mice. *Dev. Neurosci. 16:212.*
59. Lassmann, S., C. Kincaid, V. C. Asensio, and I. L. Campbell. 2001. Induction of type I immune pathology in the brain following immunization without central nervous system autoantigen in transgenic mice with astrocyte-targeted expression of IL-12. *J. Immunol. 167:5485.*
60. Ford, A. L., A. L. Goodsall, W. F. Hickey, and J. D. Sedgwick. 1995. Normal adult ramified microglia separated from other central nervous system macrophages by flow cytometric sorting. *J. Immunol. 154:4309.*
61. Carson, M. J., C. R. Reilly, J. G. Sutcliffe, and D. Lo. 1998. Mature microglia resemble immature antigen-presenting cells. *Glia 22:72.*
62. Campbell, I. L. 1998. Structural and functional impact of the transgenic expression of cytokines in the CNS. *Ann. NY Acad. Sci. 840:83.*
63. Yip, H. C., A. Y. Karulin, M. Tary-Lehmann, M. D. Hesse, H. Radeke, P. S. Heeger, R. P. Trezza, M. D. Heinzel, T. Forsthuber, and P. V. Lehmann. 1999. Adjuvant-guided type-1 and type-2 immunity: infectious/noninfectious dichotomy defines the class of response. *J. Immunol. 162:3942.*
64. Dewald, B., B. Moser, L. Barella, C. Schumacher, M. Baggiolini, and I. Clark-Lewis. 1992. IP-10, a γ-interferon-inducible protein related to interleukin-8, lacks neutrophil activating properties. *Immunol. Lett. 32:81.*
65. Campbell, I. L. 2001. Cytokine-mediated inflammation and signaling in the intact central nervous system. *Prog. Brain Res. 132:491.*
66. Luster, A. D., R. D. Cardiff, J. A. MacLean, K. Crowe, and R. D. Granstein. 1998. Delayed wound healing and disorganized neovascularization in transgenic mice expressing the IP-10 chemokine. *Proc. Assoc. Am. Physicians 110:183.*
67. Chen, S. C., G. Vassileva, D. Kinsely, S. Holzmann, D. Manfra, M. T. Wiekowski, N. Romani, and S. A. Lira. 2002. Ectopic expression of the murine chemokines CCL21a and CCL21b induces the formation of lymph node-like structures in pancreas, but not skin, of transgenic mice. *J. Immunol. 168:1001.*
68. Nakamura, K., I. R. Williams, and T. S. Kupper. 1995. Keratinocyte-derived monocyte chemoattractant protein (MCP-1): analysis in a transgenic model demonstrates MCP-1 can recruit dendritic and Langerhans cells to skin. *J. Invest. Dermatol. 105:635.*
69. Grewal, I. S., B. J. Rutledge, J. A. Fiorillo, L. Gu, R. P. Gladue, R. A. Flavell, and B. J. Rollins. 1997. Transgenic monocyte chemoattractant protein-1 (MCP-1) in pancreatic islets produces monocyte-rich insulitis without diabetes. *J. Immunol. 159:401.*
70. Fuentes, M. E., S. K. Durham, M. R. Swerdel, A. C. Lewin, D. S. Barton, J. R. Megill, R. Bravo, and S. A. Lira. 1995. Controlled recruitment of monocytes and macrophages to specific organs through transgenic expression of monocyte chemoattractant protein-1. *J. Immunol. 155:5769.*
71. Tani, M., M. E. Fuentes, J. W. Peterson, B. D. Trapp, S. K. Durham, J. K. Loy, R. Bravo, R. M. Ransohoff, and S. A. Lira. 1996. Neutrophil infiltration, glial reaction, and neurological disease in transgenic mice expressing the chemokine N51/KC in oligodendrocytes. *J. Clin. Invest. 98:529.*
72. Chen, S.-C., M. W. Leach, Y. Chen, X.-Y. Cai, L. Sullivan, M. Wiekowski, B. J. Hartman-Dovey, A. Zlotnik, and S. A. Lira. 2002. Central nervous system inflammation and neurological disease in transgenic mice expressing the CC chemokine CCL21 in oligodendrocytes. *J. Immunol. 168:1009.*
73. Lider, O., R. Hershkoviz, and S. G. Kachalsky. 1995. Interactions of migrating T lymphocytes, inflammatory mediators, and the extracellular matrix. *Crit. Rev. Immunol. 15:271.*
74. Taub, D. D., T. J. Sayers, C. R. D. Carter, and J. R. Ortaldo. 1995. α and β chemokines induce NK cell migration and enhance NK-mediated cytolysis. *J. Immunol. 155:3877.*
75. Hirsch, S., and S. Gordon. 1983. Polymorphic expression of a neutrophil differentiation antigen revealed by monoclonal antibody 7/4. *Immunogenetics 18:229.*
76. Gordon, S., L. Lawson, S. Rabinowitz, P. R. Crocker, L. Morris, and V. H. Perry. 1993. Antigen markers of macrophage differentiation in murine tissues. *Curr. Top. Microbiol. Immunol. 181:1.*
77. Shive, C. L., H. Hofstetter, L. Arrendoto, C. Shaw, and T. G. Forsthuber. 2000. The enhanced antigen-specific production of cytokines induced by pertussis toxin is due to clonal expansion of T cells and not to altered effector functions of long-term memory cells. *Eur. J. Immunol. 30:2422.*
78. Murphy, P. M. 1997. Neutrophil receptors for interleukin-8 and related CXC chemokines. *Semin. Hematol. 34:311.*
79. Michalec, L., B. K. Choudhury, E. Postlewait, J. S. Wild, R. Alam, M. Lett-Brown, and S. Sur. 2002. CCL7 and CXCL10 orchestrate oxidative stress-induced neutrophilic lung inflammation. *J. Immunol. 168:846.*
80. Gasperini, S., M. Marchi, F. Calzetti, C. Laudanna, L. Vincentini, H. Polsen, M. Murphy, F. Liao, J. M. Farber, and M. A. Cassatella. 1999. Gene expression and production of the monokine induced by IFN-γ (MIG), IFN-inducible T cell α chemoattractant (I-TAC), and IFN-γ-inducible protein-10 (IP-10) chemokines by human neutrophils. *J. Immunol. 162:4928.*
81. Hestdal, K., F. W. Ruscetti, J. N. Ihle, S. E. W. Jacobsen, C. M. Dubois, W. C. Kopp, D. L. Longo, and J. R. Keller. 1991. Characterization and regulation of RB6-8C5 antigen expression on murine bone marrow cells. *J. Immunol. 147: 22.*
82. Chiu, F.-C., and J. E. Goldman. 1985. Regulation of glial fibrillary acidic protein (GFAP) expression in CNS development and in pathological states. *J. Neuroimmunol. 8:283.*
83. Bignami, A., D. Dahl, and D. C. Rueger. 1980. Glial fibrillary acidic protein (GFA) in normal neural cells and in pathological conditions. *Adv. Cell. Neurobiol. 1:285.*
84. Brett, F. M., A. P. Mizisin, H. C. Powell, and I. L. Campbell. 1995. Evolution of neuropathologic abnormalities associated with blood-brain barrier breakdown in transgenic mice expressing interleukin-6 in astrocytes. *J. Neuropathol. Exp. Neurol. 54:766.*